Supplementary materials

Using RGB photography from a drone to monitor indicator variables of tropical-forest-ecosystem degradation

Kyuho Lee , Stephen Elliott, Pimonrat Tiansawat

Figure S1. (Left) red-black ground-marker placed in the center of circular sample plots, (Right) red-black ground marker, detected by drone image sensing.
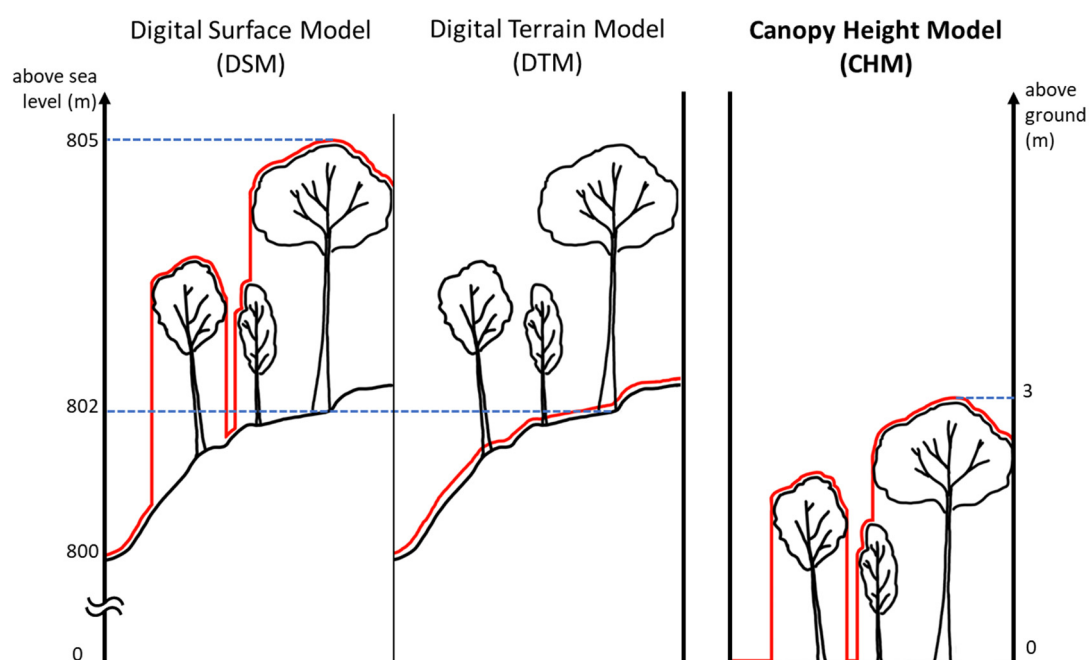

Figure S2. The canopy height model (CHM, right) was derived by subtracting the digital terrain model (DTM, centre)) from the digital surface model (DSM, left)
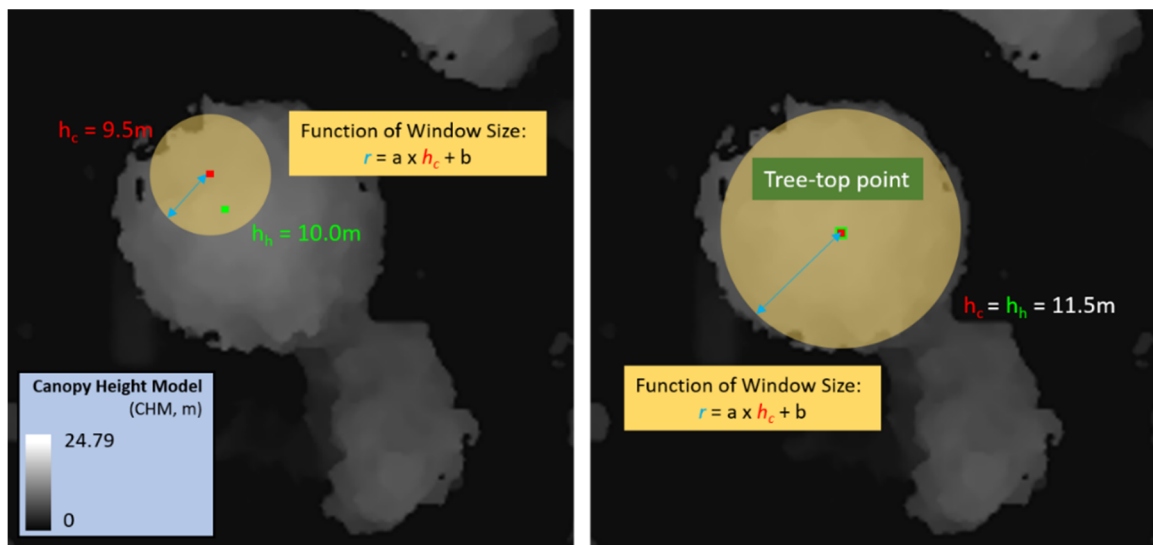
Figure S3. Explanation of the variable window-filter algorithm, used to detect tree-top points. When there is another point, higher than the center point (hh > hc) in the window, the center point is rejected as the tree-top point. When the center point is the highest point (hc = hh) in the window, the point is assigned as the tree-top point. Abbreviations: hc—height of the center point that the algorithm is currently inspecting; hh—highest point in the window (transparent yellow circle in the figure); r—radius, determined from the formular in the yellow box.
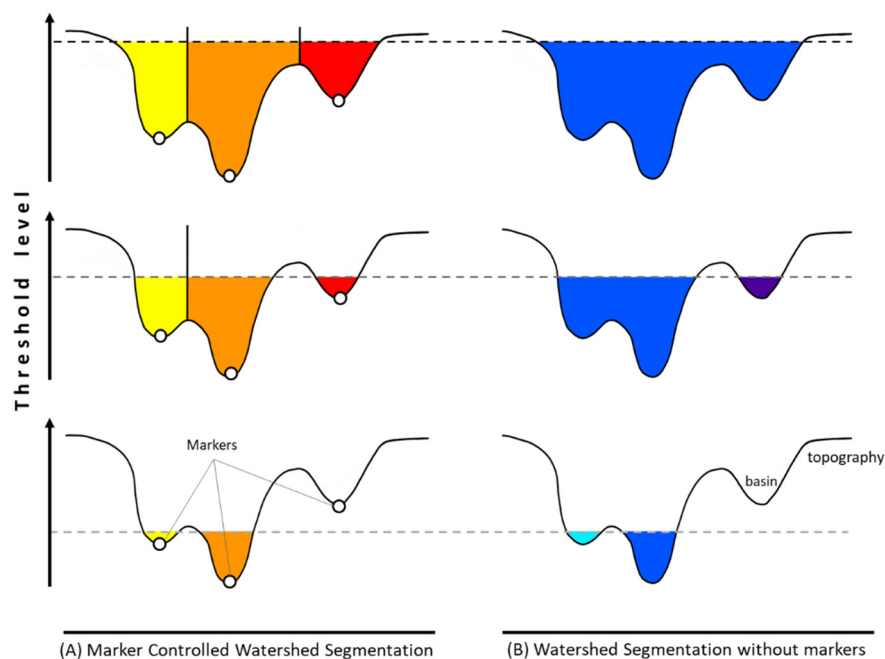

Figure S4. Principle of marker-controlled watershed segmentation (mcws) algorithm, delineating crown boundaries (adopted from Fisher, 2014 [44]).

Legend:
- ▼ Plot points, GPS detected
- ◇ Plot points, visible on drone camera
- ◇ Subpoints, visible on drone camera
- — Estimation, Stadia method
- • Plot points, Stadia method

0 1 2 3 4 5 m

Figure S5. Examples of stadia method and comparisons with GPS-detected points in orthophoto. (Left) Plot point was visible on drone-derived image (actual plot point; red square) and estimated using stadia method (red point) from visible subpoint (pink square). Two points were closer than the distance between GPS detection (grey triangle) and actual plot point. (Right) ground marker was not visible, and plot point was estimated using stadia method. Stadia method was applied in three sites, where it was necessary.

Table S1. Drone flight records, weather conditions and flight-mission settings when capturing aerial RGB images (50 m above ground). (BMSM): Ban Mae Sa Mai; (ML): Mon Long; (BPK): Ban Pong Krai; (BMM): Ban Meh Me; (LP): Lampang.

Site	Date YY-MM-DD	Flight Time	Weather Condition	Plot locations referencing	No. of pictures	Flight mission setting		
						Overlap (%)	Average Distance Between Flight Paths	Drone Speed
BMSM	20-11-04	11:37 - 11:51	Heavy clouds under strong sunlight, strong windy (c. 9.6 km/h).	Ground marker + Stadia method	283	75 %	19.0 m	12 km/h
ML	20-11-09	10:13 - 10:32	Moderate cloudy, weak wind.	Ground marker + Stadia method	335	76 %	18.2 m	12 km/h
BPK	20-10-24	15:48 - 16:10	Sunny with low solar altitude, weak wind.	Ground marker + Stadia method	335	75 %	19.0 m	13 km/h
BMM	20-06-13	11:38 - 11:51	Sunny with high solar altitude, weak wind	Ground marker	205	80 %	15.2 m	10 km/h
LP	20-09-26	13:07 - 13:21	Sunny with high solar altitude, weak wind	Ground marker	228	80 %	15.2 m	10 km/h

Table S2. Summary of ground survey data (mean values averaged across ground plots, N=8-10, see Figure 2): Ban Mae Sa Mai (BMSM), Mon Long (ML), Ban Pong Krai (BPK), Ban Meh Meh (BMM) and Lampang (LP).

Site	Tree-stocking density (tree/ha)	Canopy Cover (%)	Ground Vegetation (%)	Exposed soil + rock (%)	Mean height (m)	ACD (MgC/ha)
BMSM	3833.333	10.51	86.50	3.88	9.62	30.46
ML	2884.615	9.08	74.78	22.66	2.56	34.13
BPK	1320.513	7.78	67.66	32.11	0.23	7.91
BMM	576.9231	3.04	4.97	91.21	3.82	0.10
LP	176.2821	1.76	5.51	69.48	25.01	0.07